

# A Novel Miniaturized Reconfigurable Microstrip Antenna Based Printed Metamaterial Circuitries for 5G Applications

Hayder H. Al-Khaylani<sup>1</sup>, Taha A. Elwi<sup>2, 3, \*</sup>, and Abdullahi A. Ibrahim<sup>1</sup>

**Abstract**—A novel reconfigurable sub-6 GHz microstrip patch antenna operating at three resonant frequencies 3.6, 3.9, and 4.9 GHz is designed for 5G applications. The proposed antenna is constructed from metamaterial (MTM) array with a matching circuit printed around a printed strip line. The antenna is excited with a coplanar waveguide to achieve an excellent matching over a wide frequency band. The proposed antenna shows excellent performance in terms of  $S_{11}$ , gain, and radiation pattern that are controlled well with two photo resistance. The proposed antenna shows different operating frequencies and radiation patterns after changing the of photo resistance status. The main antenna novelty is achieved by splitting the main lobe that tracks more than one user at the same resonant frequency. Nevertheless, the main radiation lobe can be steered to the desired location by controlling the surface current motion using two varactor diodes on a matching circuit.

## 1. INTRODUCTION

A rapid demand increase for high data rates with enhanced bandwidth has developed several generations of mobile communication infrastructures to copy those 5G applications [1]. One of the most critical key points of developing any wireless communication network is antenna development that has a great impact on the bandwidth limitations and radiation properties [2]. Thus, 5G networks introduced the use of novel antenna structures based smart feature to fulfil the requirement of high data rates with the desired latency level reduction [3]. Later, several designs reported are to enhance the antenna gain-bandwidth products for the 5G communication networks requirements [4]. Most of these developed antennas are developed at the sub-6 GHz to be integrated on printed circuit board (PCB) for smart portable devices [5]. Thus, such antennas with enhanced gain-bandwidth product could be a quite strong signal toward the user side [6]. For example, a microstrip antenna structure based on metamaterial inclusions was introduced to produce an antenna forming through controlling the surface field intensity with two photo resistors [7]. Another design was proposed in [8] to control the antenna gain using a reconfigurable MTM layer with circularly polarized patch antenna for Wi-Fi and 5G applications. In [9], a fractal based MTM antenna was proposed for modern communication systems based on a reconfigurable frequency band. The proposed antenna structure in [10] was developed for biomedical application; in this antenna, the authors designed a microstrip antenna based on a hexagon MTM patch. The authors in [11] designed a flexible microstrip antenna based on an MTM rectangular patch based on a reconfigurable structure with two PIN diodes and a varactor diode. The developed antenna in [12] was proposed for 5G applications by steering the antenna radiation pattern dynamically with frequency changing.

---

*Received 15 February 2022, Accepted 26 April 2022, Scheduled 5 May 2022*

\* Corresponding author: Taha Ahmed Elwi (taelwi82@gmail.com).

<sup>1</sup> Electrical and Computer Engineering Department, Graduate School of Science, Altinbas University, Istanbul, Turkey. <sup>2</sup> Department of Communication Engineering, Al-Ma'moon University College, Baghdad, Iraq. <sup>3</sup> International Applied and Theoretical Research Center (IATRC), Baghdad Quarter, Iraq.

In this work, a printed microstrip antenna based on MTM inclusions is proposed for 5G and other modern applications within the sub-6 GHz bands. The antenna consists of a printed microstrip line with discontinuity gaps connected to a T-stub resonator. The proposed microstrip line is coupled to four fractal MTM unit cells and two matching circuits based on spiral structure. The antenna is fed with a coplanar waveguide and controlled with two varactor diodes and two photo resistors. The rest of the paper is organized as: The antenna geometrical details are presented in Section 2. The design methodology is discussed in Section 3. The results validation and discussion are theorized in Section 4. The paper is concluded in Section 5.

## 2. ANTENNA DESIGN AND GEOMETRICAL DETAILS

The proposed antenna design is based on four Moore fractal MTM unit cells with a coplanar waveguide feed, microstrip line, matching load circuits, and T-stubs as seen in Figure 1(a). Four Moore fractal unit cells have been utilized in the proposed antenna to increase the antenna size reduction and realize multiband resonances [13]. The antenna is printed on an FR4 Techtronic epoxy substrate with dimensions of  $62 \times 40 \text{ mm}^2$ . A bandwidth enhancement can be achieved within a limited area by magnifying surface current that is afforded on electrically long path [14]. The coplanar waveguide is used to avoid the capacitive coupling between antenna patch and the ground plane [15]. Nevertheless, such a design maintains the other surface of the antenna substrate without any printed circuit to be used for busing electronic circuit [16]. The transmission line is designed with the width of (0.6) to realize  $50 \Omega$  matching circuit and to transfer the surface current motion to the proposed Moor structure [17]. The gap on the transmission line is introduced to force the current motion toward the fractal geometry as explained in [16]. The matching circuit is introduced to avoid surface wave retardation that could be created in an opposite interference and inductive loss due to the use of the transmission line junction that can be removed by the capacitive effects of the matching circuit [18]. The proposed T-stub is introduced to suppress the surface waves from the antenna edges that negatively affects the radiation efficiency [19]. The microstrip patch is printed on an FR4 substrate without a ground plane. The substrate dielectric constant is 4.3 with a height of 1.67 mm. Two photo resistors are used in antenna structure to get different operating frequencies and radiation patterns by switching photo resistors ON/OFF.

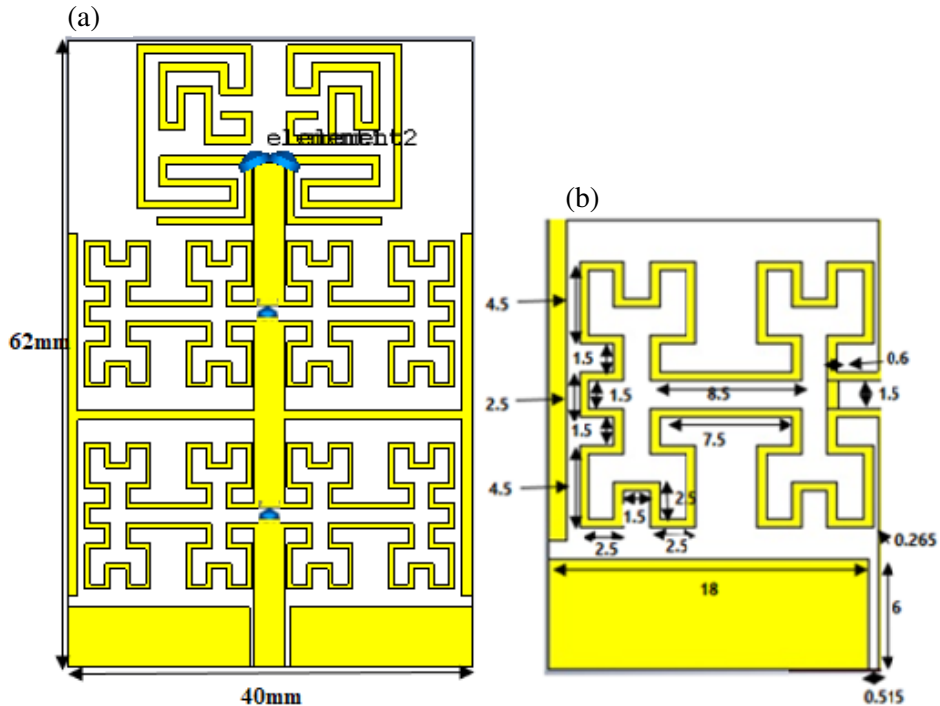


**Figure 1.** Antenna geometrical details: (a) front view and (b) MTM unit cell.

### 3. DESIGN METHODOLOGY

In this section, the authors apply a parametric study based on simulation analysis of the proposed antenna design parameters. In such analysis, the influences of introducing the antenna parts to the performance are considered too. We focus on the effects of those parameters and parts on the antenna  $S_{11}$  and gain spectra. The main targeted frequency bands in our design are 3.9 GHz and 4.9 GHz because they are very applicable with 5G frequency bands [5]. The simulation analysis is conducted using CST MWS software package [20]. For this, the analysis is attempted in this section to arrive at the optimal design as follows.

#### 3.1. Transmission Line Design

For the parametric analysis purposes, the authors changed the transmission line length from 40 mm to 60 mm with respect to monitoring  $S_{11}$  spectra only. Such analysis is conducted to ensure the effects of changing the transmission line length. Figure 2 shows  $S_{11}$  for three different lengths of the transmission line (40, 50, 60) mm. The authors choose 50 mm as a transmission line length which is located at 3.8 GHz with  $S_{11}$  of  $-25$  dB and gain of 3.1 dBi.

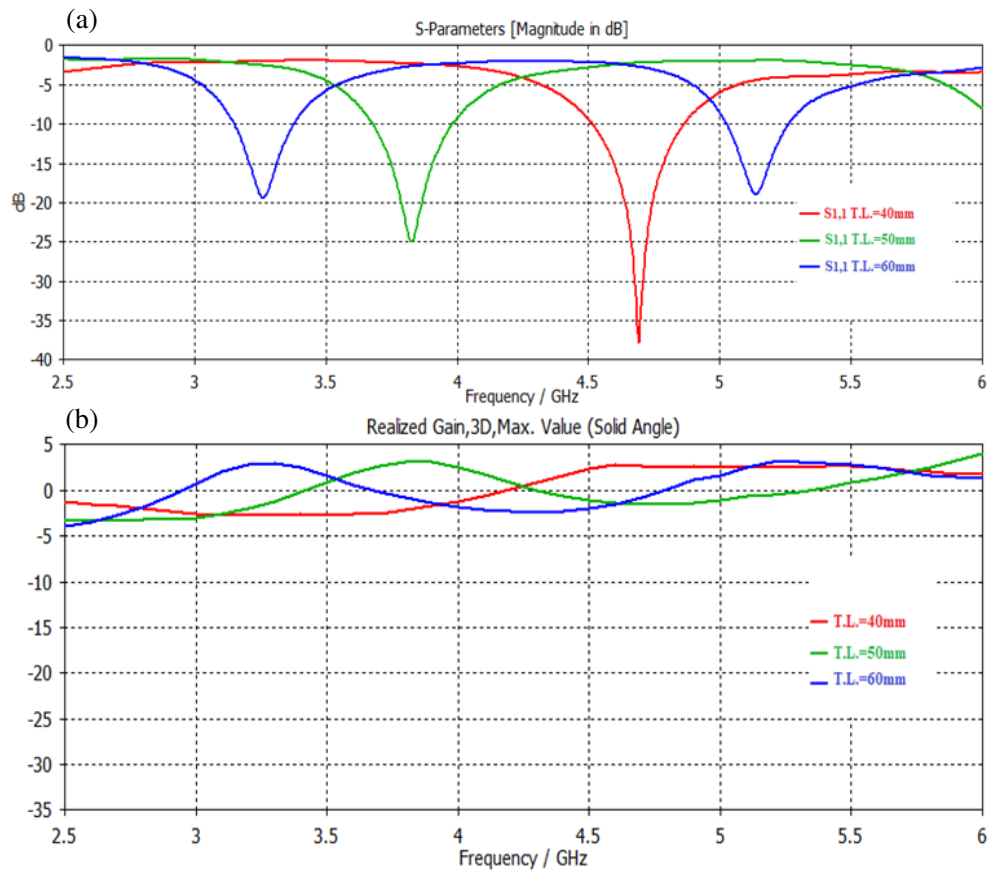


**Figure 2.** Antenna performance: (a)  $S_{11}$  and (b) gain spectra.

#### 3.2. Unit Cell Effects

The proposed antenna design is structured from Moore fractal geometry. In this design, two Moore cells are filed in the proposed antenna substrate. Therefore, to study the effects of adding them to the antenna performance, the authors applied a parametric study based on CST MWS. In this simulation, the authors included the first Moore unit cell to the antenna design, then compared the obtained results

to the identical antenna design based on two Moore cells. We found, at the first scenario, that the antenna showed multiple frequency bands within the frequency range of interest. However, after introducing the other Moore unit cell, the antenna introduced different frequency bands with the range of frequency of interest. This is achieved because the connection between the unit cells on the proposed transmission line is in series. In such connection, the current motion is mostly in the same direction of the proposed unit cells. Nevertheless, the combination between them is in series connection resulting in adding the effects of them directly to each other. Since the proposed unit cell is capacitive inclusion, adding them to increase their number may realize a significant reduction in the equivalent capacitor [8], which in turn increases the particular operating frequency band [9]. For more details about the current motion, the authors present the surface current motion on the proposed Moore unit cell in Figure 3.

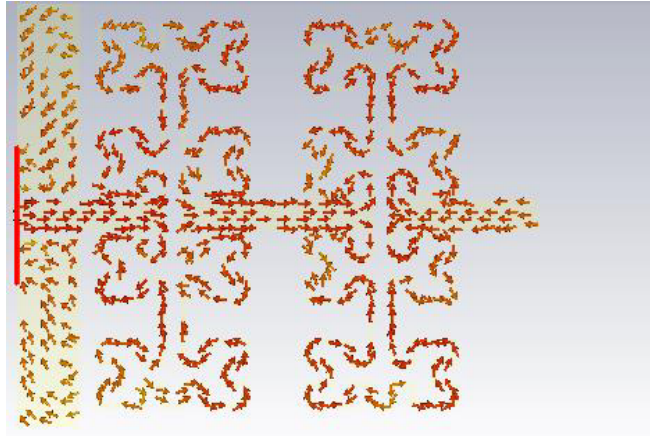


**Figure 3.** Current motion on the proposed unit cell.

For that, the authors present the relative electromagnetic properties, in terms of permittivity and permeability, of the proposed unit cell in Figure 4. It is found that the proposed unit cell provides near zero permittivity and permeability within the frequency band of interest. Such observation reveals that the proposed unit cell is an excellent candidate to magnify the surface current; this is by reducing the reactive parts on the antenna patch to increase the antenna bandwidth [11].

### 3.3. T Junction Effects

This section shows the effect of T junction on antenna performance. It works to split the main antenna radiation beam to increase the number of receiving users from the same antenna at same resonance frequency [5]. Nevertheless, such a property realizes the main requirement of the beam forming in the 5G devices. For this work,  $S_{11}$  and gain values after adding the MTM unit cell are found as  $-23.6$  dB and  $-15.84$  dB at 3.55 GHz and 3.8 GHz, respectively, with the gain of  $-0.897$  dBi at 3.55 GHz and 3.48 dBi at 3.8 GHz, respectively. These observations are presented in Figure 5 for the evaluated  $S_{11}$  and gain spectra.

### 3.4. Gap Effects

The gap on the transmission line is introduced to derive the current motion toward the fractal geometry. This section describes the effect of gaps on the characteristics of the antenna including the resonance frequency,  $S_{11}$ , gain, and radiation pattern properties. This is analyzed numerically by controlling the photo resistor status at 3.6 GHz represented by a variable resistor with light incidence as shown in Table 1.

Figure 6 shows the evaluated  $S_{11}$  spectra of the proposed antenna with different cases conditions of the used photo resistors. A significant effect is found on  $S_{11}$  spectra due to switching the photo resistors conduction as described in Table 1.

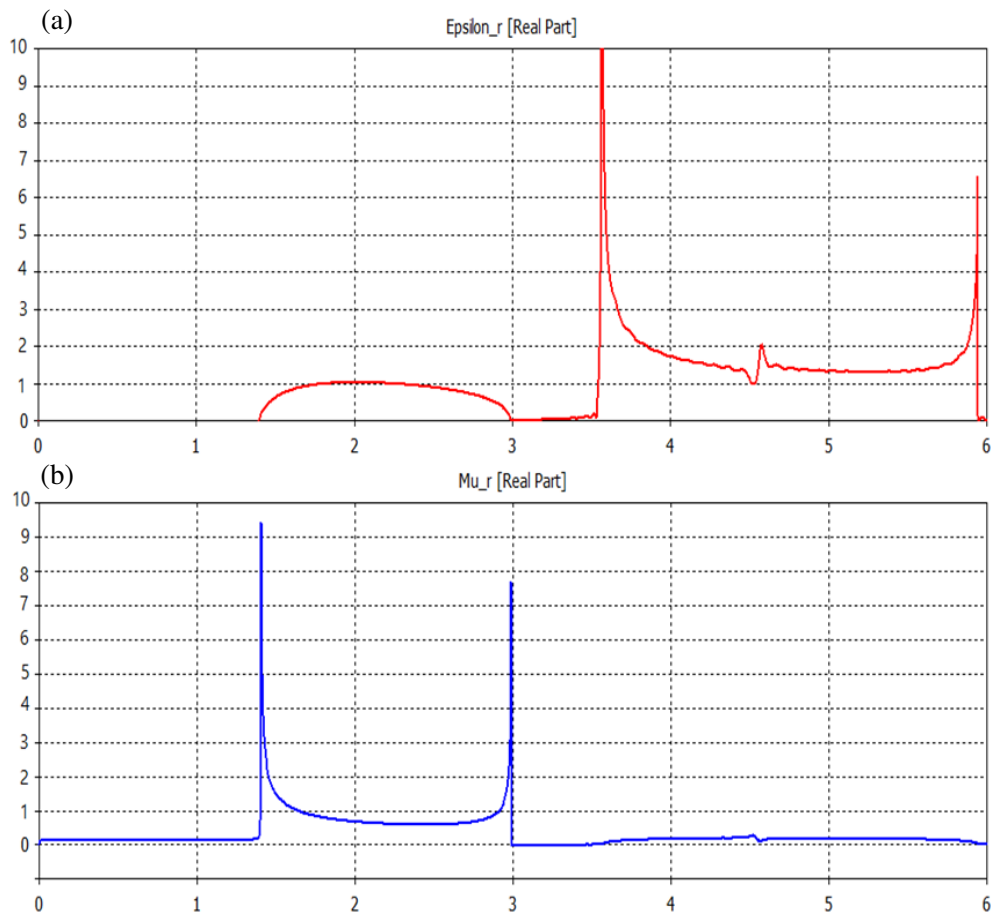


**Figure 4.** Relative electromagnetic properties of the proposed unit cell: (a) permittivity and (b) permeability.

**Table 1.** Antenna performance with respect of varying the photo resistors conductions.

Case	R <sub>1</sub>	R <sub>2</sub>	Gain	Main lobe direction	Angular beam width
1	0	0	3.36	162°	61.2°
2	0	1	2.88	150°	52.3°
3	1	0	3.43	167°	68.1°
4	1	1	2.9	149°	53.1°

### 3.5. Matching Circuit Effects

Directing the main antenna lobes to the desired location can be achieved by controlling the surface current motion on the antenna patch. In this work, a variable capacitive load is introduced to increase the surface current magnitude to a certain direction [7]. In such a case, the antenna portion with less capacitance takes less time to radiate the electromagnetic energy from the other side with higher capacitor value. Another benefit of matching circuit load is to mitigate side lobe of the antenna and improves the gain at 4.9 GHz. For this, the varactor diodes are introduced to matching circuit to control the antenna radiation at 4.9 GHz to the desired location as shown in Table 2.

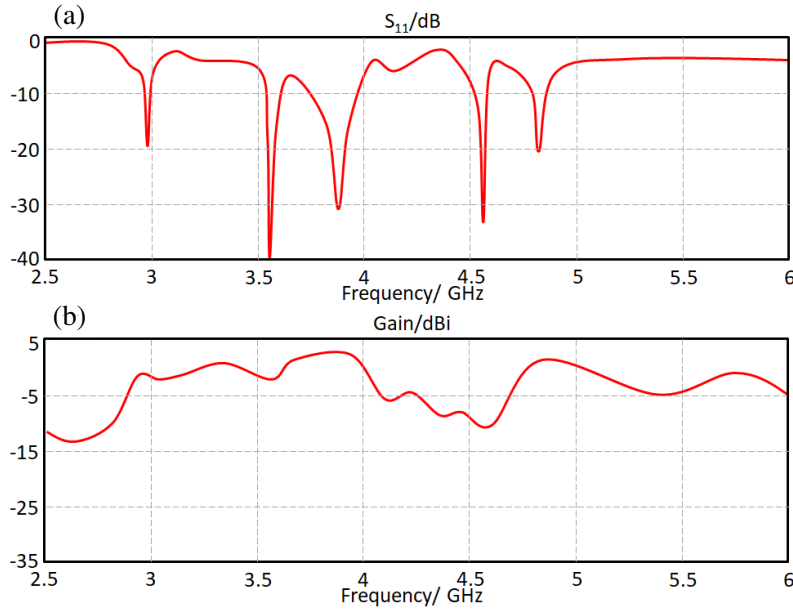


**Figure 5.** Antenna performance after introducing the proposed MTM unit cell: (a)  $S_{11}$  and (b) gain spectra.

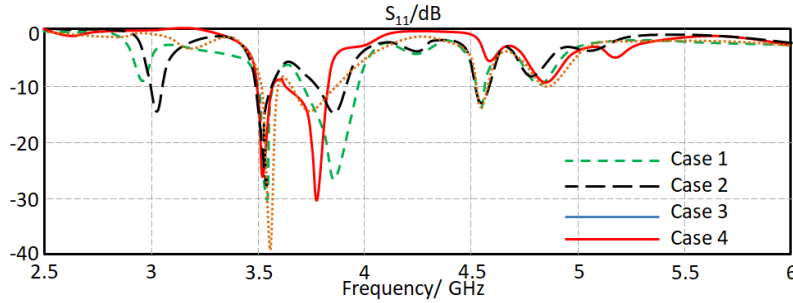


**Figure 6.** Antenna performance in terms of  $S_{11}$  spectra with varying the photo resistors conditions.

**Table 2.** Antenna main lobe direction with respect of varying the varactor diodes.

Varactor Diodes	Main Lobe Direction (Photo Resistance)			
	Case1 (00)	Case2 (01)	Case3 (10)	Case4 (11)
1 pF	-2	1	-141	130
5 pF	-176	-179	-147	128
10 pF	-175	-178	-150	127

#### 4. EXPERIMENTAL VALIDATION

In this section, before conducting the antenna fabrication, the authors applied a numerical simulation based on HFSS software package [21] for further validation. The obtained results from the two software packages agree very well. Next, the proposed antenna is fabricated using chemical deposition process as seen in Figure 7(a). In this work, the antenna is tested experimentally using a vector network analyzer 37347A and a microwave chamber. We experimentally evaluated the antenna performance in terms of

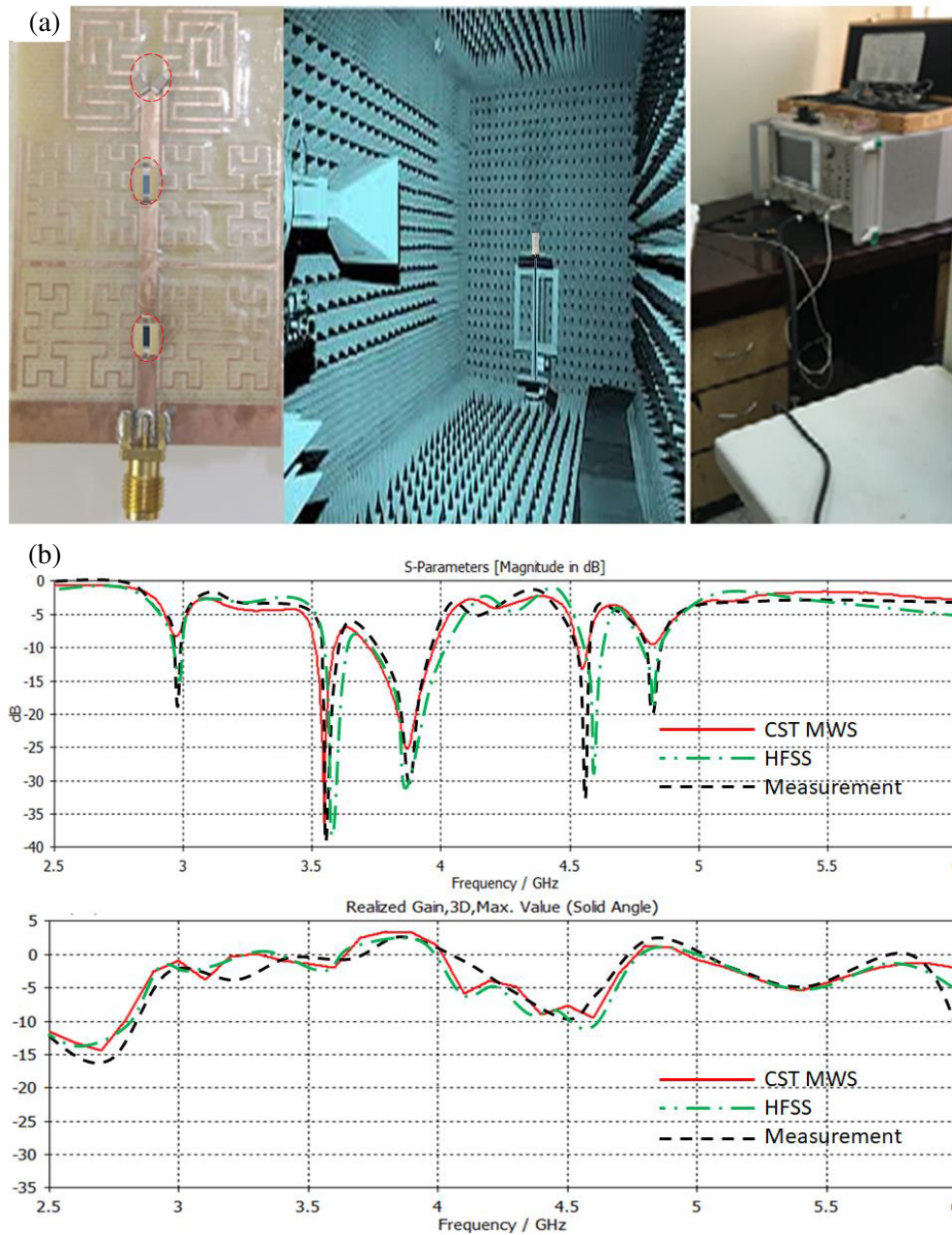


**Figure 7.** Antenna performance in terms of  $S_{11}$  and gain spectra validations: (a) fabricated prototype and measurement setup and (b) measurement results.

$S_{11}$  and Gain ( $G_o$ ) spectra as seen in Figure 7(b). It is found that the proposed antenna provides more than single frequency resonance ( $f_r$ ) at 3.9 GHz and 4.9 GHz with  $G_o$  of 3 dB and 3.5 dB, respectively, without including the photo resistor and/or the varactor diodes switching effects.

Then, the measured and simulated radiation patterns at the 3.6 GHz and 4.9 GHz are shown in Figure 8. The radiation pattern measurements are done inside an RF anechoic chamber with respect to the diodes switching. For these measurements, the authors conducted the measurements after switching diodes ON and OFF according to the considered cases: 00, 01, 10, and 11. It is found that the proposed antenna radiation patterns beam width and main lobe directivity are changed significantly with the diodes switching.

Finally, the proposed antenna performance is compared to those published in the literature. The

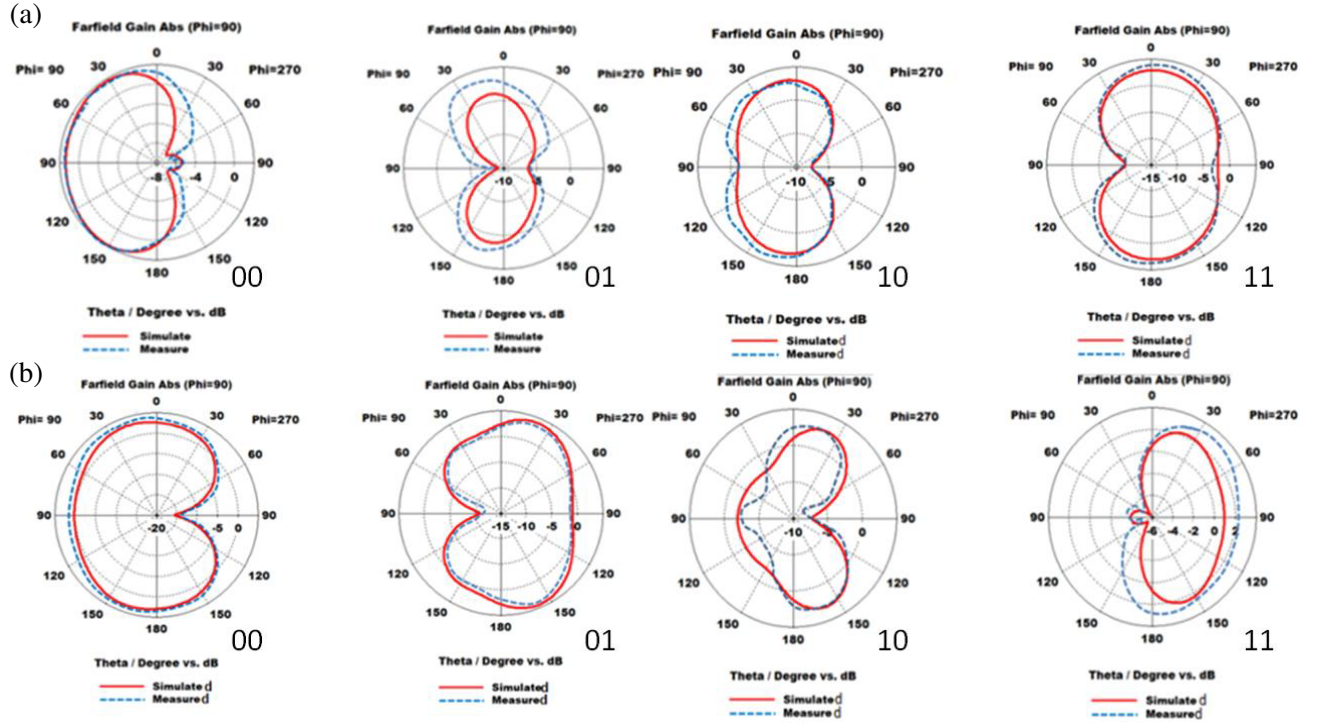


**Figure 8.** Measured and simulated radiation patterns at: (a) 3.6 GHz and (b) 4.9 GHz.

**Table 3.** Comparison between the proposed work performance and other published results in the literature.

Ref.	$f_r$ /GHz	Substrate	$G_o$ /dBi	Size/mm	Reconfiguration process	Diodes No.
[1]	3.5, 3.8	FR4	2.3	$10.7 \times 22.5 \times 1.6$	No	uncontrolled
[2]	3.5	FR4 epoxy	5	$25.2 \times 48 \times 1.6$	No	uncontrolled
[3]	2.45, 3.5, 5.2	FR4	3.4	$39 \times 37 \times 1.6$	Frequency	1
[4]	2, 3.4, 2.4, 3.1	FR4	1.98	$37 \times 35 \times 1.6$	Frequency	2
[5]	2.1, 2.45, 3.2, 3.5	FR4	2.2	$37 \times 35 \times 1.6$	Frequency	2
[6]	2.55, 3.5, 4.75	Teflon	3	$47 \times 19$	No	uncontrolled
[7]	3.31–6.03	Glass epoxy	2	$25 \times 25 \times 1$	Frequency	3
This work	3.9, 4.9	FR4	3, 3.5	$62 \times 40 \times 1.6$	Beam forming and frequency	2

comparison is attempted in terms of antenna size, substrate type, frequency resonance, gain, and reconfiguration process. We found that the proposed antenna realizes an excellent beam forming with frequency reconfiguration. Nevertheless, the proposed antenna realizes that at two frequency bands as listed in Table 3.

## 5. CONCLUSION

This work is proposed to design a reconfigurable antenna based on radiation pattern and frequency reconfiguration for 5G applications. The reconfiguration process is applied using two varactor diodes to steer the antenna radiation pattern toward the desired direction. However, the antenna frequency reconfiguration is realized using two photo resistors to control the antenna bands. We found that the proposed antenna provides excellent matching at the frequency bands of 3.9 GHz and 4.9 GHz with gain

of 3 dBi and 3.5 dBi, respectively. Such gain enhancement is obtained by conducting Moore MTM unit cells to a T junction resonator that reduces the reactive part of the antenna which in turn increases the antenna gain. Finally, the antenna is fabricated and tested experimentally to be compared to the simulated results. The comparison results show excellent agreements between the simulated and measured ones.

## REFERENCES

1. Shafique, K., B. A. Khawaja, F. Sabir, S. Qazi, and M. Mustaqim, "Internet of Things (IoT) for next-generation smart systems: A review of current challenges, future trends and prospects for emerging 5G-IoT scenarios," *IEEE Access*, Vol. 8, 23022–23040, 2020.
2. Rappaport, T. S., Y. Xing, O. Kanhere, S. Ju, A. Madanayake, S. Mandal, A. Alkhateeb, and G. C. Trichopoulos, "Wireless communications and applications above 100 GHz: Opportunities and challenges for 6G and beyond," *IEEE Access*, Vol. 7, 78729–78757, 2019.
3. Zhou, L., Y. Jiao, Y. Qi, Z. Weng, and L. Lu, "Wideband ceiling-mount omnidirectional antenna for indoor distributed antenna systems," *IEEE Antennas Wirel. Propag. Lett.*, Vol. 13, 836–839, 2014.
4. Singhal, S. and A. K. Singh, "Modified Star-Star Fractal (MSSF) super-wideband antenna," *Microw. Opt. Technol. Lett.*, Vol. 59, 624–630, 2017.
5. Waladi, V., N. Mohammadi, Y. Zehforoosh, A. Habashi, and J. Nourinia, "A novel Modified Star-Triangular Fractal (MSTF) monopole antenna for super-wideband applications," *IEEE Antennas Wirel. Propag. Lett.*, Vol. 12, 651–654, 2013.
6. Manohar, M., "Miniaturised low-profile super-wideband Koch snowflake fractal monopole slot antenna with improved BW and stabilised radiation pattern," *IET Microw. Antennas Propag.*, Vol. 13, 1948–1954, 2019.
7. Hussein, M. I., A. Hakam, and M. Ouda, "Planar ultra-wideband elliptical antenna for communication applications," *Proceedings of the 2016 IEEE Wireless Communications and Networking Conference*, 1–5, Doha, Qatar, April 3–6, 2016.
8. Liang, X.-L., S.-S. Zhong, and W. Wang, "Elliptical planar monopole antenna with extremely wide bandwidth," *Electron. Lett.*, Vol. 42, 441–442, 2006.
9. Yan, X.-R., S.-S. Zhong, and X.-L. Liang, "Compact printed semi-elliptical monopole antenna for super-wideband applications," *Microw. Opt. Technol. Lett.*, Vol. 49, 2061–2063, 2007.
10. Manohar, M., U. K. Nemani, R. S. Kshetrimayum, and A. K. Gogoi, "A novel super wideband notched printed trapezoidal monopole antenna with triangular tapered feedline," *Proceedings of the 2014 International Conference on Signal Processing and Communications (SPCOM)*, 1–6, Bangalore, India, July 22–25, 2014.
11. Manohar, M., R. S. Kshetrimayum, and A. K. Gogoi, "A compact dual band-notched circular ring printed monopole antenna for super wideband applications," *Radioengineering*, Vol. 26, 64–70, 2017.
12. Dong, Y., W. Hong, L. Liu, Y. Zhang, and Z. Kuai, "Performance analysis of a printed super-wideband antenna," *Microw. Opt. Technol. Lett.*, Vol. 51, 949–956, 2009.
13. Wang, Z., Y. Dong, and T. Itoh, "Transmission line metamaterial-inspired circularly polarized RFID antenna," *IEEE Antennas Wirel. Propag. Lett.*, Vol. 19, 964–968, 2020.
14. Cao, W., W. Ma, W. Peng, and Z. N. Chen, "Bandwidth-enhanced electrically large microstrip antenna loaded with SRR structures," *IEEE Antennas Wirel. Propag. Lett.*, Vol. 18, 576–580, 2019.
15. Xu, L. and Y. J. Zhou, "Low profile high-gain antenna for broadband indoor distributed antenna system," *Appl. Comput. Electromagn. Soc. J. (ACES)*, Vol. 35, 791–796, 2020.
16. Xu, H.-X., G.-M. Wang, J.-G. Liang, M. Q. Qi, and X. Gao, "Compact circularly polarized antennas combining meta-surfaces and strong space-filling meta-resonators," *IEEE Trans. Antennas Propag.*, Vol. 61, 3442–3450, 2013.
17. Abdulsattar, R. K., T. A. Elwi, and Z. A. Abdul Hassain, "A new microwave sensor based on the moore fractal structure to detect water content in crude oil," *Sensors*, Vol. 21, 7143, MDPI, 2021.

18. Alaukally, M. N. N., T. A. Elwi, and D. C. Atilla, "Miniaturized flexible metamaterial antenna of circularly polarized high gain-bandwidth product for radio frequency energy harvesting," *Int. J. Commun. Syst.*, 2021.
19. Ali, D., T. A. Elwi, and S. Ozbay, "Metamaterial-based printed circuit antenna for biomedical applications," *European Journal of Science and Technology*, Vol. 26, 12–15, 2021.
20. [www.cst.com](http://www.cst.com).
21. [www.ansoft.com](http://www.ansoft.com).